Metallomics

PAPER

View Article Online
View Journal

Cite this: DOI: 10.1039/c9mt00225a

Comprehensive and comparative exploration of the *Atp7b*$^{-/-}$ mouse plasma proteome†

Maud Lacombe,[a] Michel Jaquinod,[a] Lucid Belmudes,[a] Yohann Couté,[a] Claire Ramus,[a] Florence Combes,[a] Thomas Burger,[ab] Elisabeth Mintz,[c] Justine Barthelon,[d] Vincent Leroy,[d] Aurélia Poujois,[e] Alain Lachaux,[f] France Woimant[e] and Virginie Brun *[a]

Received 9th September 2019,
Accepted 2nd December 2019

DOI: 10.1039/c9mt00225a

rsc.li/metallomics

Wilson's disease (WD), a rare genetic disease caused by mutations in the *ATP7B* gene, is associated with altered expression and/or function of the copper-transporting ATP7B protein, leading to massive toxic accumulation of copper in the liver and brain. The *Atp7b*$^{-/-}$ mouse, a genetic and phenotypic model of WD, was developed to provide new insights into the pathogenic mechanisms of WD. Many plasma proteins are secreted by the liver, and impairment of liver function can trigger changes to the plasma proteome. High standard proteomics workflows can identify such changes. Here, we explored the plasma proteome of the *Atp7b*$^{-/-}$ mouse using a mass spectrometry (MS)-based proteomics workflow combining unbiased discovery analysis followed by targeted quantification. Among the 367 unique plasma proteins identified, 7 proteins were confirmed as differentially abundant between *Atp7b*$^{-/-}$ mice and wild-type littermates, and were directly linked to WD pathophysiology (regeneration of liver parenchyma, plasma iron depletion, *etc.*). We then adapted our targeted proteomics assay to quantify human orthologues of these proteins in plasma from copper-chelator-treated WD patients. The plasma proteome changes observed in the *Atp7b*$^{-/-}$ mouse were not confirmed in these samples, except for alpha-1 antichymotrypsin, levels of which were decreased in WD patients compared to healthy individuals. Plasma ceruloplasmin was investigated in both the *Atp7b*$^{-/-}$ mouse model and human patients; it was significantly decreased in the human form of WD only. In conclusion, MS-based proteomics is a method of choice to identify proteome changes in murine models of disrupted metal homeostasis, and allows their validation in human cohorts.

Significance to metallomics

Wilson's disease (WD) is a genetic disorder resulting in toxic copper accumulation in the liver and brain. In this study, we used discovery and targeted MS-based proteomics to identify proteins present at different concentrations in the plasma of a mouse model of WD compared to wild type mice. Evaluation in plasma samples from WD patients and healthy donors confirmed differential expression for 2 proteins: ceruloplasmin and alpha-1 antichymotrypsin.

Introduction

Wilson's disease (WD) is a rare genetic disorder affecting approximately 1/30 000 new-borns; it is characterised by toxic copper accumulation in the liver and brain. WD is a monogenic autosomal-recessive condition resulting from mutations in the *ATP7B* gene located on chromosome 13 in humans. More than 600 different mutations of the *ATP7B* gene have been described, associated with reduced expression or functional impairment of ATP7B protein, a copper-transporting P-type ATPase essential to maintaining copper homeostasis.[1] This 164 kDa trans-membrane protein is expressed at high levels in hepatocytes in the trans-Golgi

[a] *Univ. Grenoble Alpes, CEA, Inserm, IRIG, BGE, 38000 Grenoble, France. E-mail: virginie.brun@cea.fr; Fax: +33 4 38 78 50 51; Tel: +33 4 38 78 96 57*
[b] *CNRS, BIG-BGE, F-38000 Grenoble, France*
[c] *Univ. Grenoble Alpes, CEA, CNRS, IRIG, LCBM, 38000 Grenoble, France*
[d] *Clinique Universitaire d'Hépato-gastroentérologie, Centre Hospitalier Universitaire Grenoble, Grenoble, France*
[e] *National Reference Centre for Wilson's Disease, AP-HP, Lariboisière University Hospital, Paris, France*
[f] *National Reference Centre for Wilson's Disease, Hôpital Femme Mère Enfant, Hospices Civils de Lyon, Lyon, France*

† Electronic supplementary information (ESI) available: Table S1. See DOI: 10.1039/c9mt00225a

network where it delivers copper cofactor to cuproenzymes, such as ceruloplasmin, before they are secreted into plasma. In response to increased cellular copper concentrations, ATP7B translocates to the endo-lysosomal compartment and the plasma membrane of bile canaliculi to promote copper efflux into the bile.[2] In WD, perturbation of ATP7B protein expression, stability, function, or intracellular targeting impair copper delivery to the secretory pathway and copper excretion into the bile. Disruption of copper homeostasis causes massive copper accumulation in hepatocytes, leading to irreversible oxidative damage and, ultimately, cell death. A massive release of free copper (unbound to ceruloplasmin) into the bloodstream is then observed which contributes to extending the free copper overload and toxicity throughout the body, particularly in the central nervous system.

Although the genetic mutations causing WD are present even before birth, clinical symptoms usually only appear during childhood or teenage years. WD is primarily hepatic with a wide spectrum of manifestations, spanning from a slight (clinically undetectable) elevation of transaminases to acute liver failure, acute-on-chronic hepatitis, and cirrhosis. Neurological symptoms including tremors, dysarthria, dystonia, or Parkinsonian symptoms may dominate initially or appear gradually as the liver disease progresses. These neurological disorders are often associated with psychiatric disorders (depression, anxiety).[3] The ''Kayser–Fleisher ring'' is a specific ocular symptom of WD resulting from copper accumulation around the cornea; it is present in 95% of patients with neurological symptoms.[1]

Therapeutic management of WD patients requires lifelong administration of copper-chelating agents and/or zinc salts to reduce intestinal copper absorption. Liver transplantation is necessary to treat fulminant hepatitis or decompensated liver cirrhosis. As the more serious symptoms appear later, earlier detection of WD would allow early initiation of pharmacological treatments, before patients develop hepatic and neurological diseases alongside irreversible organ damage. However, because of its low incidence, its variable clinical presentations, and the lack of a single 100% reliable diagnostic parameter that can exclude or confirm the diagnosis of WD, early detection remains challenging. WD is thus generally only confirmed following a combination of biological, ophthalmological (recognition of ''Kayser–Fleisher ring''), brain MRI, and genetic tests. In combination with classical liver function tests, specific biological assays have been developed to detect decreased serum ceruloplasmin concentrations and increased urinary copper excretion.[1,3] Recently, assays measuring exchangeable serum copper and relative exchangeable copper were also proposed to improve WD diagnosis.[4,5] In addition to biological investigations, molecular characterisation of the *ATP7B* gene can reveal disease-specific mutations or haplotypes. Most WD patients are mixed heterozygotes (carrying two different *ATP7B* gene mutations) and the relationship between the *ATP7B* genotype and the disease phenotype has proven difficult to decipher. Additional epigenetic, environmental and genetic factors (*e.g.* other genes involved in copper metabolism) are likely to strongly influence WD pathogenesis and clinical phenotype.[6–8] To facilitate WD diagnosis and as part of a plan to screen new-borns, Jung and coworkers[9] recently proposed a targeted proteomic assay that directly quantifies ATP7B in dried blood spots (DBS). Promising results were obtained, with DBS from 12 WD patients showing reduced concentrations or lack of ATP7B. However, the authors warned that complementary biological tests remain necessary to diagnose patients carrying mutations which have a functional impact without affecting ATP7B expression levels.[9]

In addition to the search for new diagnostic tests, attempts have been made to study the pathophysiology of WD, and thus to facilitate the development of new therapeutic compounds. For example, in 1999, Buiakova and coworkers[10] developed the *Atp7b*$^{-/-}$ mouse model. This model is now well-established as a genetic and phenotypic model for the hepatic form of WD. In this murine model, stop codons were introduced into exon 2 of the *ATP7B* gene, resulting in the production of a truncated mRNA and suppression of ATP7B expression in the liver. Like WD patients, *Atp7b*$^{-/-}$ mice accumulate copper in the liver, excrete copper in their urine and progressively develop liver disease.[11] Copper overload is also observed in other organs (such as kidney and brain) at later stages, although neurological symptoms are generally not observed in *Atp7b*$^{-/-}$ mice. Without chelation therapy, liver disease in *Atp7b*$^{-/-}$ mice progresses through the major successive stages. Liver disease is absent and no histological evidence of the disease is observed up to 8–12 weeks after birth, although underlying molecular changes alter the cell cycle machinery and lipid metabolism.[12,13] After 12 weeks, signs of hepatocellular injury are present, with hepatocyte necrosis and lobular inflammation. Bile duct proliferation is also observed alongside metabolic modifications. From 28 weeks of age, liver inflammation and fibrosis are observed alongside regenerating parenchyma and proliferating bile ducts.[11,13]

In an attempt to gain new insights into the pathophysiological changes associated with WD and with a view to identifying new biomarkers to facilitate diagnosis, we investigated the plasma proteome modifications associated with liver disease development in the *Atp7b*$^{-/-}$ mouse model. As most plasma proteins are secreted by the liver, we hypothesised that the disruption of copper homeostasis and subsequent liver dysfunction in the *Atp7b*$^{-/-}$ mouse could significantly affect the plasma proteome. To characterise the quantitative modifications occurring in the plasma proteome in *Atp7b*$^{-/-}$ mice compared to wild-type (WT) *Atp7b*$^{+/+}$ littermates, we first conducted a label-free quantitative (LFQ) mass spectrometry (MS)-based discovery proteomics study. To confirm the modifications detected, we developed a targeted quantitative proteomics assay using liquid chromatography-selected reaction monitoring (LC-SRM). This assay was applied to plasma samples from a distinct, larger, cohort of *Atp7b*$^{-/-}$ and WT mice. Using this strategy, we identified seven plasma proteins expressed at differential abundances between *Atp7b*$^{-/-}$ and WT mice. We then went on to determine their relevance to human disease, by investigating these proteins in clinical samples from WD patients, non-alcoholic steatohepatitis (NASH) patients, and healthy donors.

Experimental

Mice and plasma samples

The *Atp7b*$^{-/-}$ mouse model used in this study was developed by Buiakova *et al.*[10] 129S6/SvEv *Atp7b*$^{-/-}$ males were crossed with C57BL/6J WT females before embryo transfer into recipient female mice. *Atp7b*$^{+/-}$ heterozygous mice (maintained on a mixed 129S6/SvEv x C57BL/6J genetic background) were bred in our animal care facility and used to generate *Atp7b*$^{-/-}$ and *Atp7b*$^{+/+}$ mice. This breeding scheme prevents death of *Atp7b*$^{-/-}$ mice shortly after birth due to copper deficiency. Indeed, *Atp7b*$^{-/-}$ mice are born copper-deficient and delivery of copper from the mammary gland to the milk is impaired in *Atp7b*$^{-/-}$ mothers. Breeding, genotyping, and all experimental procedures were performed according to protocols approved by the ethics committees (C2EA – 12 Comité d'éthique ComEth Grenoble and C2EA – 44 CETEA – CEA DSV IdF), the veterinary authorities, and the French Ministry for Research.

Blood samples were collected in sodium heparin-treated tubes (Becton Dickinson) by cardiac puncture from *Atp7b*$^{-/-}$ and WT mice (males and females) of various ages (Table 1). Blood samples were immediately stored at 4 °C. Within one hour of collection, they were centrifuged at 2000*g* and 4 °C for 15 min to collect plasma supernatants, which were aliquoted and immediately stored at −80 °C.

Patients and plasma samples

Plasma samples from 20 WD patients (13 women and 7 men, mean age: 41 ± 12 years) were collected at the French Reference Centre for Wilson's disease (Lyon and Paris, France). Plasma samples from 10 NASH patients (5 women and 5 men, mean age: 49 ± 8 years) and 10 healthy subjects with no history of chronic liver disease (5 women and 5 men, mean age 45 ± 13 years) were collected at the Clinique Universitaire d'Hépato-gastroentérologie (Grenoble, France). The study protocols were approved by the ethics committee (Comité d'Evaluation Ethique de l'Inserm CEEI/IRB and Grenoble hospital's institutional review board). All patients gave written informed consent for their participation in this study. Plasma samples were collected by vein puncture and using lithium heparin-treated or EDTA-treated tubes (Becton Dickinson). Previous proteomics studies indicated that detection of the proteins targeted in this study is not influenced by anticoagulant.[14–16] Blood samples were stored at 4 °C for up to one hour before centrifugation at 2000*g* and 4 °C for 15 min to isolate plasma. Plasma samples were anonymised, aliquoted and stored at −80 °C until use. Clinical data and biological parameters for the 30 recruited patients are presented in Table S1 (ESI†).

Biochemical preparation of plasma samples

Plasma samples were prepared by a protocol adapted from the MED-FASP (multiple enzyme digestion – filter aided sample preparation) protocol.[17] For each sample, 3 μL of plasma was loaded onto a 10 kDa cut-off ultrafiltration device (Amicon). Plasma proteins were denatured and reduced on the device by adding 4 M urea, 25 mM ammonium bicarbonate and 10 mM TCEP. Each sample was washed twice with 4 M urea, 50 mM ammonium bicarbonate and then alkylated with 55 mM iodoacetamide in 4 M urea, 25 mM ammonium bicarbonate. After two additional washing steps, the sample volume was reduced to 25 μL and proteins were digested for 3 h at 37 °C using trypsin/LysC mix (Promega) at a protein/enzyme ratio of 1 : 20 (w/w). The urea concentration was reduced to 1 M by dilution, and digestion was allowed to proceed for a further 3 h at 37 °C. Proteolytic peptides were recovered by adding 50 μL NaCl 0.5 M to the filter and centrifuging for 40 min at 14 000*g* at room temperature. When performing targeted proteomics analyses, defined concentrations of isotope-labelled peptides (crude Pepotec grade, Thermo Fischer Scientific) were spiked into the digested samples at this stage of the protocol (see Table 2). All peptide digests were purified on Macrospin C18 columns (Harvard apparatus) in line with the manufacturer's recommendations before drying by vacuum centrifugation.

NanoLC-MS/MS analyses

Dried peptide digests were solubilised in 2 mL of 5% acetonitrile, 0.1% formic acid; 1 μL (equivalent to ≈100 ng protein) of this solution was analysed by nanoflow liquid chromatography (nanoLC) coupled online to MS (Ultimate 3000 and LTQ Orbitrap Velos Pro, Thermo Scientific). Peptides were sampled on a 300 μm × 5 mm PepMap C18 precolumn and separated on a 75 μm × 250 mm C18 column (Pepmap, Thermo Fischer). The nanoLC method consisted in a 120 min gradient at a flow rate of 300 nL min^{-1}, ranging from 5% to 37% acetonitrile in 0.1% formic acid for 114 min, followed by a ramp up to 72% acetonitrile in 0.1% formic acid for the last 6 min. MS and MS/MS data were acquired using Xcalibur (Thermo Fisher Scientific). The spray voltage was set to 1.4 kV, and the heated capillary was maintained at 200 °C. Survey full-scan MS spectra (m/z = 400–1600) were acquired in the Orbitrap at a resolution of 60 000 after the accumulation of 10^6 ions (maximum filling time: 500 ms). The 20 most intense ions from the preview survey scan delivered by the Orbitrap were fragmented by collision-induced dissociation (collision energy: 35%) in the linear trap (LTQ) after accumulation of 10^4 ions (maximum filling time: 100 ms).

Table 1 Groups and numbers of mice used for LFQ proteomics discovery analysis, and validation based on targeted proteomics

		Genotype and sex of mice			
		Atp7b$^{-/-}$		*Atp7b*$^{+/+}$ (WT)	
Type of study	Age of mice	Female	Male	Female	Male
Discovery using LFQ nanoLC-MS/MS	36 weeks	4	4	1	3
	44 weeks	3	2	2	2
Validation using isotopically labeled peptides and LC-SRM	From 12 weeks to 56 weeks	12	12	15	9

Table 2 Proteins assayed by targeted proteomics

		Proteomics discovery analysis		Targeted proteomics evaluation		
Uniprot ID	Protein names	log_2FC	Adjusted *p*-value	Signature peptides	FC	*p*-Value (Mann–Whitney)
Q61650	Beta-globin	−7.84	0.006	Not assessed by LC-SRM		
Q3UBS3	Haptoglobin	−3.79	0.026	AEGDGVYTLNDEK DITPTLTLYVGK	0.21	0.264
Q03734	Serine protease inhibitor A3M	−1.92	0.024	FSISTDYNLK	0.36	0.003
Q8BK48	Carboxylesterase 2E	1.54	0.026	LGVLGFFSTGDQHAK IIPGVVDGEFLPK	2.09	0.002
Q80SX2	C4b-binding protein alpha-chain	1.56	0.00004	PEVGNGTLSDEK	1.04	0.409
Q3UPK6	Proteasome subunit alpha type	1.58	0.009	Not assessed by LC-SRM		
E9Q414	Apolipoprotein B-100	1.59	0.042	ADLSGLYSPIK SLPVGNTVFDLNK LQVATANNVSPYIK	1.12	0.078
Q3TWK8	Fibulin-1	1.60	0.0005	Not assessed by LC-SRM		
A0A0R4J032	Complement component 9	1.68	0.015	TSNFNADFALK FSATEVPEK ALPTSYEK	2.21	0.0001
Q9WVJ3	Carboxypeptidase Q	1.69	0.037	Not assessed by LC-SRM		
Q3UBR4	Cathepsin S	1.69	0.005	YIQLPFGDEDALK	1.54	0.014
Q5SU94	FMS-like tyrosine kinase 4	1.69	0.0004	GPVLEATAGDELVK	1.79	0.003
P01592	Immunoglobulin J chain	1.83	0.0005	IIPSTEDPNEDIVER IVVPLNNR	2.83	0.00003
D3Z6T3	Cathepsin E	2.23	0.00002	Not assessed by LC-SRM		
Q922B3	Intercellular adhesion molecule 1	2.41	0.000005	TFDLPATIPK LDTPDLLEVGTQQK ADGALLPIGVVK	1.57	0.0006
Q542D9	Transferrin receptor, isoform CRA	3.38	0.0000006	LNSIEFADTIK AGEITFAEK TAAEVAGQLIIK	5.17	0.00001
P07361	Alpha-1-acid glycoprotein 2	3.93	0.000003	WFFIGAAVLNPDYR YVGGVK IFADLIVLK	1.85	0.003
Q8BK56	Alpha-fetoprotein	6.02	0.0003	THPNLPVSVILR	371.05	0.0005
Q549A5	Clusterin	*1.03*	*0.009*	SLLNSLEEAK ELLQSFQSK LFDSDPITVVLPEEVSK	2.03	0.00006
Q61147	Ceruloplasmin	*−0.3324*	*0.286*	VFFEQGATR DTANLFPHK	0.80	0.030

Processing nanoLC-MS/MS data

Raw data were processed using MaxQuant software (version 1.5.8.3). Spectra were searched against the UniProt database (*Mus musculus* taxonomy) and the frequently observed contaminants database embedded in MaxQuant. Trypsin/LysC was selected as the enzyme, and up to two missed cleavages were allowed. Precursor mass error tolerances were set to 20 ppm and 4.5 ppm for initial and main searches, respectively. Peptide modifications allowed during the search were: carbamidomethylation (C, fixed), acetyl (Protein N-term, variable) and oxidation (M, variable). Minimum peptide length was set to seven amino acids. Minimum number of peptides, razor + unique peptides and unique peptides were all set to 1. Maximum false discovery rates (FDR) – calculated by employing a reverse database strategy – were set to 0.01 at both peptide and protein levels. Intensity-based absolute quantification (iBAQ) values were calculated from MS intensities of unique + razor peptides. The MS proteomics data have been submitted to the ProteomeXchange Consortium *via* the PRIDE partner repository[18] under dataset identifier PXD011007. Statistical analyses were performed using ProStaR.[19] Proteins identified in the reverse and contaminant databases and proteins identified by a single peptide, as well as proteins for which fewer than 4 iBAQ values were available in a single condition, were removed from the list. After log_2 transformation, iBAQ values were normalised by median centring before imputing missing values (missing values were replaced by the 2.5 percentile value for each sample); statistical testing was performed using a Limma moderated *t*-test. Differentially recovered proteins were sorted out using a log_2 fold-change (FC) cut-off of 1.5 (between *Atp7b*$^{-/-}$ and WT mice samples) and a *p*-value threshold (on the remaining proteins) that guarantees a Benjamini–Hochberg FDR < 5%.

LC-SRM analyses

The peptides monitored during targeted analyses were selected based on: (i) sequence-specificity by BLAST search against UniProt database (*Mus musculus* or *Homo sapiens* taxon), (ii) analytical detectability predicted based on their ESPPredictor score,[20] (iii) absence of post-translational modifications, and (iv) absence of reactive amino acid residues (C, M, N-terminal Q). SRM transition lists used to monitor the selected signature peptides were generated using Skyline.[21] Labelled versions of the selected signature peptides (crude Pepotec grade) with C-terminal [$^{13}C_6$,$^{15}N_2$]-lysine or C-terminal [$^{13}C_6$,$^{15}N_4$]-arginine were purchased from Thermo Scientific. These isotopically labelled peptides were spiked into pre-digested plasma and

analysed by LC-SRM to experimentally select the most responsive SRM transitions, optimise the LC gradient, and schedule acquisition. For optimal detection, two distinct LC-SRM acquisitions were performed when analysing murine plasma samples: (i) the first targeted alpha-fetoprotein, soluble transferrin receptor 1, carboxylesterase 2, complement C9, immunoglobulin J chain, and SERPINA3M; (ii) the second targeted clusterin and ceruloplasmin (Table S1, ESI†).

LC-SRM analyses were performed on a 6500 QTrap hybrid triple quadrupole/linear ion trap mass spectrometer (AB Sciex) with a TurboV electrospray ion source. Data were processed using Analyst software (version 1.6, AB Sciex). The mass spectrometer was linked to an Ultimate 3000 LC-chromatography system (Thermo Scientific). Chromatographic separation was achieved using a two-solvent system combining solvent A (2% acetonitrile, 0.1% formic acid) and solvent B (80% acetonitrile, 0.1% formic acid). Before separation, peptide digests were concentrated on a C18 precolumn (Phenomenex, ref: AJO-8782). Peptides were separated on a Kinetex C18 column (2.1 mm ×100 mm, core–shell 2.6 μm, 100 Å, Phenomenex, ref: 00D-4462-AN) by applying a linear gradient from 4% to 14% B in 27 min, from 14% to 35% B in 8 min, and from 35% to 90% B in 4 min at a flow rate of 60 μL min^{-1}. MS data were acquired in positive mode with an ion-spray voltage of 4100 V; curtain gas was used at 45 p.s.a. and the interface heater temperature was set to 250 °C. Collision cell exit, declustering and entrance potentials were set to 21, 55 and 14 V, respectively. Collision energy (CE) values were calculated using linear equations based on the unlabelled peptide precursor m/z ratios: CE = 0.044 m/z + 5 and CE = 0.05 m/z + 4 (Volts) for doubly- and triply-charged precursors, respectively, and the same CE was used for both labelled and unlabelled versions of each signature peptide. The analyses combined in the same run: (1) a precursor ion scan between 400 and 1000 m/z as a survey scan for Information-Dependent Acquisition (IDA), (2) an Enhanced Product Ion (EPI) scan with a scan speed of 1000 amu s^{-1} and a dynamic fill-time for optimal MS/MS analysis, (3) an SRM acquisition with Q1 and Q3 quadrupoles operating at unit resolution. The acquisition time window for scheduled SRM analyses was set to 120 s, and the target scan time was set to 1.5 s. With a mean base width of 20 s, 13 points were acquired per LC peak. The MS proteomics data have been deposited to the ProteomeXchange Consortium *via* the PRIDE partner repository[18] under dataset identifier PXD011007.

LC-SRM data processing

LC-SRM data were analysed using Skyline software.[21] Peak picking was performed using the mProphet algorithm and the ''second best peak'' model. A Q-value of 0.01 (1% FDR) was set as the cut-off for peptide signal analysis. In addition to peptide signal scoring, all transitions were visually inspected and excluded if they were incompatible with quantification (low signal-to-noise ratio, obvious interference). Unlabelled/labelled peak area ratios were calculated for each SRM transition and were averaged to determine the corresponding peptide ratio. At least two transition pairs were used to determine biomarker concentrations. Protein ratios were calculated from the ratios obtained for signature peptides. Finally, candidate biomarker concentrations were calculated from the average protein ratio and the concentration of isotope-labelled peptide added to the sample, as estimated by the provider. Plasma protein concentrations determined using LC-SRM were compared between groups of mice. For each protein, statistical significance was evaluated on the basis of a FC > 2 or < -2 and a p-value < 0.05 (Mann–Whitney test). Significance of protein concentration differences in human plasma samples was analysed by one-way ANOVA, followed by the Tukey multiple-comparison *post hoc* test. The threshold for significance was set to $p < 0.05$.

ELISA assays

Alpha-fetoprotein (FETA) and carboxylesterase 2 (CES2) concentrations in human plasma samples were determined using the alpha-fetoprotein ELISA kit (reference ab193765, Abcam) and the CES2 ELISA kit (reference ABIN420902, Cloud-clone corp), respectively, according to the manufacturers' instructions.

Results

Discovery LFQ proteomics to explore the *Atp7b*$^{-/-}$ mouse plasma proteome

We initially characterised and compared the plasma proteomes of *Atp7b*$^{-/-}$ and WT mice using unbiased LFQ proteomics. For this discovery phase, plasma samples from 8 WT mice and 13 *Atp7b*$^{-/-}$ mice were collected from 36- and 44-week-old animals (Table 1). In this age range, *Atp7b*$^{-/-}$ mice had a 50-fold higher intrahepatic copper concentration than WT mice. *Atp7b*$^{-/-}$ mice also exhibited advanced liver disease with intense inflammation and fibrosis (as previously described[5]). Plasma samples were prepared using an adapted MED-FASP protocol and were analysed by nanoLC-MS/MS (Fig. 1A). Data processing using two significant peptides per protein and an FDR of less than 1% at both peptide and protein levels resulted in the identification of 367 unique proteins in the 21 plasma samples (Table S1, ESI†).

To assess differences in plasma protein abundance between *Atp7b*$^{-/-}$ and WT mice, a Limma test (with $\log_2$FC > 1.5 or < -1.5 and p-value < 0.05) was applied to the LC-MS/MS dataset. Upon applying these parameters, 18 of the 367 unique proteins were identified as differentially abundant between the two groups of mice. Of these proteins, 15 were enriched in *Atp7b*$^{-/-}$ plasma samples, and the remaining three were more abundant in WT plasma samples (Fig. 1B and Table 2). Interestingly, plasma levels of ceruloplasmin were not found to differ between *Atp7b*$^{-/-}$ and WT mice.

Targeted quantitative proteomics to validate changes to the *Atp7b*$^{-/-}$ mouse plasma proteome

Following the discovery phase, a quantitative LC-SRM assay was developed to confirm the differential abundance of the selected proteins on a distinct set of plasma samples collected from 24 *Atp7b*$^{-/-}$ and 24 WT mice aged between 12 and 56 weeks (Table 1). This range of ages covers all stages of liver disease

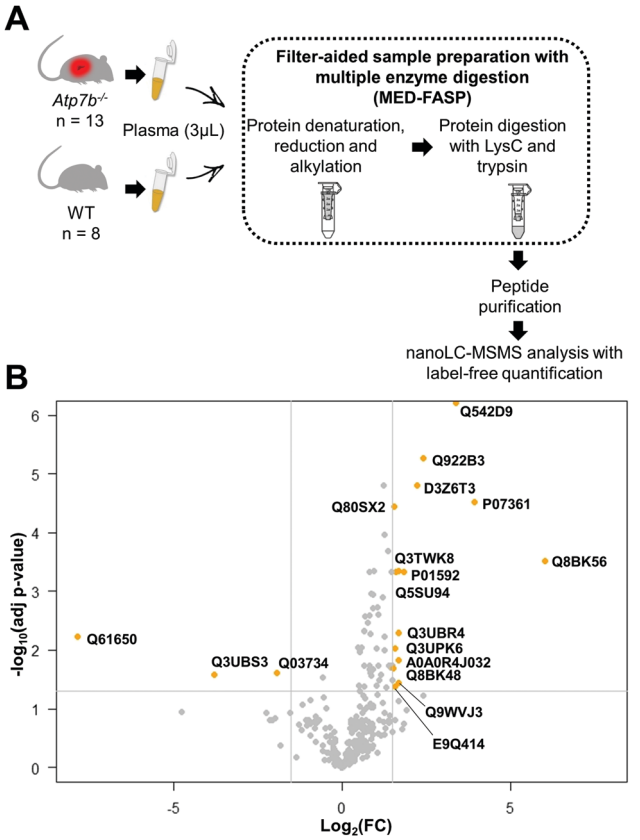

Fig. 1 Discovery proteomics workflow allowed identification of 18 differentially-expressed proteins. (A) Plasma sample preparation before discovery LFQ proteomics analysis. (B) Volcano plot showing proteins with significantly different expression levels in plasma from *Atp7b*$^{-/-}$ compared to WT mice (orange points). The $-\log_{10}$(adjusted *p*-value) was plotted against the $\log_2$ FC (*Atp7b*$^{-/-}$/WT). The non-axial vertical lines indicate ± 1.5 $\log_2$ FC; the non-axial horizontal line delimits *p*-value = 0.05 (5% FDR threshold).

progression in this model animal. The initial list of protein targets consisted of the proteins identified in the discovery phase, with the exception of beta-globin, which was excluded from the panel studied as it is affected by haemolysis. Two additional proteins were added to the list: (i) ceruloplasmin, which is a classical biological indicator used to diagnose WD in humans; and (ii) clusterin, which was included because it interacts with ATP7B[22] – although its FC in the discovery assay was 2.06 (below the cut-off), it had a very significant *p*-value (0.001; Table 2).

To develop the LC-SRM assay, the 19 target proteins were submitted to *in silico* digestion. Surrogate signature peptides were then selected for each protein based on sequence-specificity, absence of missed cleavage or post-translational modification, and analytical detectability. Then, isotopically labelled versions of the signature peptides were purchased, spiked into pre-digested plasma matrix and analysed by LC-SRM to allow us to select only the most responsive peptides and SRM transitions, and to schedule acquisition. Following these optimisations, four of the proteins selected based on the discovery phase results (proteasome subunit alpha type, fibulin-1, carboxypeptidase Q and cathepsin E) were found to be unquantifiable due to difficulties in finding specific and/or "flyer" peptides. Consequently, the final LC-SRM assay (based on two acquisition methods) included 15 target proteins, which were quantified based on monitoring of 31 signature peptides, in labelled and unlabelled forms (Table S1, ESI†).

Plasma samples from 24 *Atp7b*$^{-/-}$ and 24 WT mice were prepared by the adapted MED-FASP protocol. All samples were spiked with labelled peptides in defined quantities before peptide purification (Fig. 2A). Following LC-SRM analysis and data processing, plasma protein concentration differences were investigated with respect to sex and genotype differences. Five of the 15 plasma proteins (haptoglobin, serine protease inhibitor A3M (SERPINA3M), carboxylesterase 2E, complement component C9, and clusterin) were differentially abundant between males and females (Table S1, ESI†). Seven of the 15 plasma proteins quantified were confirmed to be differentially abundant between samples from *Atp7b*$^{-/-}$ and WT mice (Fig. 3A). Plasma concentrations for carboxylesterase 2E, transferrin receptor isoform CRA (soluble form), complement component C9, immunoglobulin J chain, alpha-fetoprotein, and clusterin were significantly higher in *Atp7b*$^{-/-}$ mice. An age-dependent increase mirroring disease progression in *Atp7b*$^{-/-}$ mice was clearly observed for transferrin receptor isoform CRA, alpha-fetoprotein, and clusterin (Fig. 3B and Table S1, ESI†). Plasma levels for SERPINA3M, a mouse orthologue of human alpha 1-anti chymotrypsin, were decreased in *Atp7b*$^{-/-}$ mice. In line with the discovery study results, plasma ceruloplasmin levels were similar in *Atp7b*$^{-/-}$ and WT mice (Fig. 3A).

Screening of biomarker candidates in WD patients

Following the identification of these seven differentially abundant plasma proteins in the *Atp7b*$^{-/-}$ mouse model, we wished

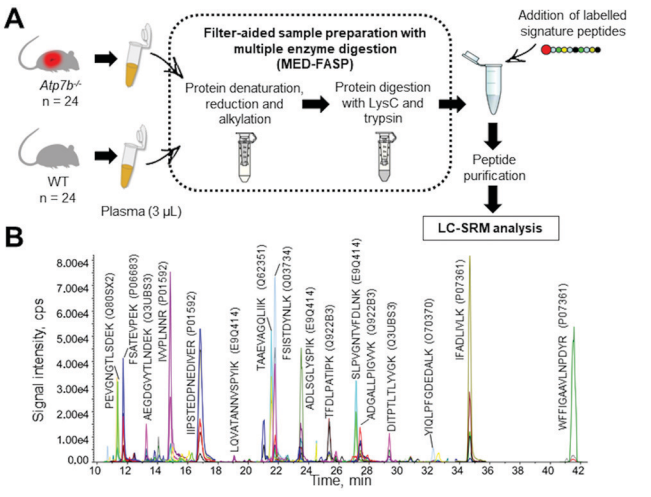

Fig. 2 Validation of 15 selected proteins in murine plasma by targeted proteomics. (A) Workflow for plasma sample preparation before targeted quantitative analysis. (B) Extracted ion chromatogram for scheduled LC-SRM analysis of plasma samples. To improve readability, only 16 of the 31 peptides monitored have been assigned on the chromatogram.

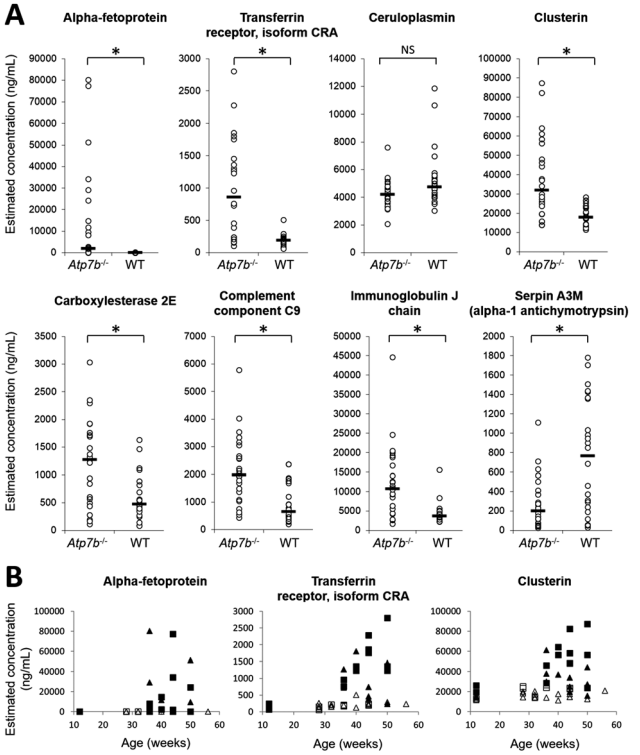

Fig. 3 Seven proteins confirmed to be expressed at significantly different levels between *Atp7b*$^{-/-}$ and WT mice. (A) Dot plots showing the concentrations of seven proteins confirmed to be differentially abundant between *Atp7b*$^{-/-}$ and WT mice, on the basis of a FC of 2 and a p-value <0.05, (Mann–Whitney test). Quantification results obtained for ceruloplasmin are also presented. (B) Age-related changes observed for alpha-fetoprotein, transferrin receptor isoform CRA, and clusterin in *Atp7b*$^{-/-}$ (filled symbols) and WT (open symbols) mice. Concentration values measured for male and female mice are distinguished by square and triangular symbols, respectively.

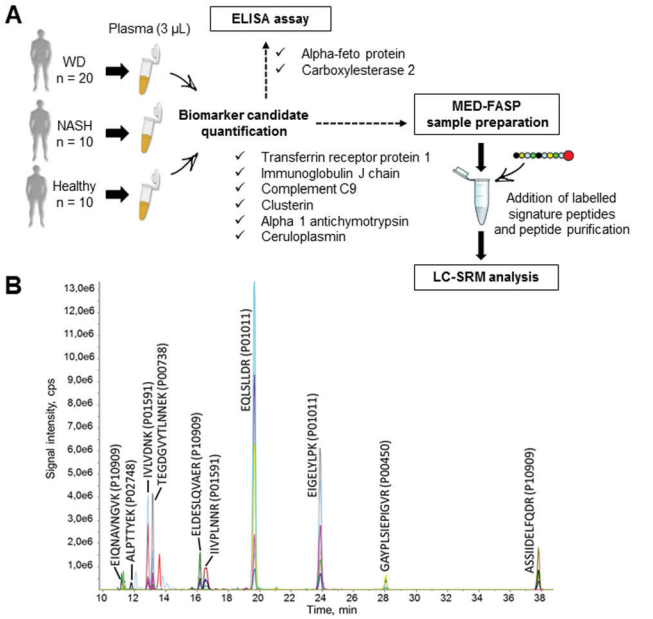

Fig. 4 Quantification of eight selected proteins in human plasma samples by targeted proteomics. (A) Workflow for plasma sample preparation before targeted quantitative analysis. (B) Extracted ion chromatogram for scheduled LC-SRM analysis of human plasma samples. To improve readability, only 10 of the 14 peptides monitored have been assigned on the chromatogram.

to investigate whether these results were transferrable to human WD. Therefore, we modified our targeted proteomic assay to allow quantification of the seven human protein orthologues in plasma samples. Ceruloplasmin was once again included in the panel assessed, as its plasma concentration is classically decreased in WD and is used for diagnosis.

As for the mouse study, signature peptides were selected for the eight target human proteins based on sequence-specificity, absence of modifiable amino acids or post-translational modifications, and analytical detectability. Labelled signature peptides were purchased and used to develop the assay (SRM transition selection, LC gradient optimisation and scheduled acquisition) (Fig. 4A and Table S1, ESI†). Following these optimisations, the ''human version'' of our LC-SRM assay was used to quantify six proteins (transferrin receptor protein 1, complement C9, immunoglobulin J chain, SERPINA3, clusterin and ceruloplasmin), which were monitored simultaneously based on levels of 14 signature peptides, present in both labelled and unlabelled versions. The transition list consisted of 80 SRM transitions (Fig. 4B). Signature peptides for the remaining two proteins, human carboxylesterase 2 and alpha-fetoprotein, were barely detectable in plasma matrix, but both proteins were readily quantified using complementary ELISA assays.

Following these analytical optimisations, we determined whether significant differences in plasma protein concentration existed between WD patients and healthy donors. The 20 WD patients were recruited by the French Reference Centres for WD. These patients presented either liver disease or a combination of hepatic, neurological, and psychiatric symptoms. Importantly, at the time of plasma sample collection, all WD patients were being treated with copper chelators (D-penicillamine, triethylenetetramine) or zinc sulfate, and their liver function was thus restored, as determined clinically and biologically based on transaminase levels and prothrombin time values (Table S1, ESI†).

To assess the specificity of protein abundance changes, the 8 plasma proteins were also measured in patients with another liver disease: NASH. NASH was selected as the control liver disease as it shares some major clinical and histological features with WD (steatosis, inflammation, fibrosis).[23]

The quantification results were analysed by one-way ANOVA analysis followed by a *post hoc* Tukey test. The plasma concentrations of 5 proteins identified in the *Atp7b*$^{-/-}$ mouse model were no different between the three groups of human subjects (Table S1, ESI†). However, the plasma concentrations of alpha 1-antichymotrypsin (SERPINA3) were significantly decreased in treated WD patients compared to healthy donors, but not different from levels measured in NASH patients. Plasma levels of carboxylesterase 2 were increased in NASH patients, but there was no significant difference between treated WD

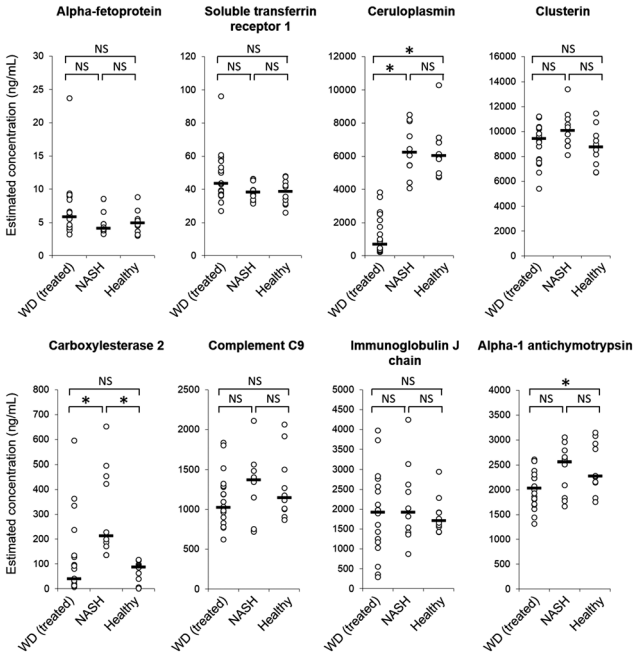

Fig. 5 Ceruloplasmin and alpha-1-antichymotrypsin expressed at significantly different levels between treated WD patients and healthy donors. Levels of 8 selected proteins were measured in treated WD patients, NASH patients and healthy donors by targeted assays. Dot plots show the concentrations of the 8 selected proteins in clinical plasma samples. Statistical analysis was based on a one-way ANOVA, followed by a Tukey multiple-comparison *post hoc* test ($p < 0.05$).

patients and healthy subjects. Finally, as expected in the human disease, plasma levels of ceruloplasmin were significantly decreased in WD patients compared to both healthy subjects and NASH patients (Fig. 5). In summary, plasma proteome changes in treated human WD were quite different to those observed in the *Atp7b*$^{-/-}$ mouse.

Discussion

In this study, we used a pipeline combining unbiased discovery and targeted quantitative proteomics to characterise the plasma proteome changes associated with disease development in the *Atp7b*$^{-/-}$ mouse, a well-established model of hepatic WD. The proteins for which changes were detected were then assayed in plasma samples from WD patients. To the best of our knowledge, this is the first study to comprehensively explore the plasma proteome of this preclinical model and to investigate the similarities and differences compared to the human disease.

Seven proteins were identified in *Atp7b*$^{-/-}$ mice for which abundance in plasma was significantly altered (more than 2-fold) compared to control littermates (Fig. 2C). Upregulation of alpha-fetoprotein, soluble transferrin receptor 1 and clusterin can clearly be linked to the pathogenic mechanisms of WD. Interestingly, plasma levels of alpha-fetoprotein were higher in *Atp7b*$^{-/-}$ than in WT mice, in line with the intense regeneration of liver parenchyma associated with disease progression.[13] We also observed increased levels of soluble transferrin receptor 1 (sTFR1) in plasma from *Atp7b*$^{-/-}$ mice, suggesting plasma iron depletion. In line with this result, Merle and coworkers[24] reported altered serum iron parameters in *Atp7b*$^{-/-}$ mice due to reduced ceruloplasmin ferroxidase activity. This reduction in activity leads to default incorporation of plasma iron into apotransferrin and impedes iron efflux from the liver to the circulation.[25] Our results indicated similar ceruloplasmin plasma levels between *Atp7b*$^{-/-}$ and WT littermates, which is consistent with the results of a previous study reporting normal serum ceruloplasmin levels in *Atp7b*$^{-/-}$ mice.[13] In contrast, the same study reported a marked alteration in the balance between apo-ceruloplasmin (inactive) and holoceruloplasmin (copper-bound) in *Atp7b*$^{-/-}$ animals.[13] We also detected a significant increase in plasma clusterin in *Atp7b*$^{-/-}$ mice. This protein has been directly linked to maintaining copper homeostasis, and is secreted by a large number of tissues including the liver. This oxidative-stress-induced protein acts as an intracellular and extracellular controller of protein homeostasis.[26] In the context of WD, Materia and coworkers[22,27] demonstrated specific molecular interactions between clusterin and ATP7B, and suggested a role for clusterin in quality control for and clearance of misfolded ATP7B.

Our results also identified four additional deregulated proteins for which the precise mechanisms relating to WD pathophysiology have yet to be deciphered. Plasma carboxylesterase 2 (isoform e) was detected at higher levels in *Atp7b*$^{-/-}$ mice. Although not fully characterised, this isoform is a member of the CES2 hydrolase family, which is involved in clearing xenobiotics and regulating lipid metabolism in the murine and human liver.[28] Soluble CES2 proteins are contained in the endoplasmic reticulum or secreted, they exhibit triacylglycerol and diacylglycerol hydrolase activity. This activity was shown to be strongly related to several metabolic diseases – including NASH – which share pathogenic and histological hallmarks with WD (liver steatosis, inflammation, and fibrosis).[29] The elevated concentration of Ces2e in *Atp7b*$^{-/-}$ mice may be linked to deregulated lipid metabolism, which has been described in this model.[12] Plasma levels of complement C9 and immunoglobulin J chain – both immune proteins – were also higher in *Atp7b*$^{-/-}$ mice. However, the precise molecular mechanisms which led to their increased plasma abundance are currently unknown. Finally, SERPINA3M, a murine orthologue of human alpha 1-anti chymotrypsin (AACT),[30] is a typical acute phase protein, circulating levels of which dramatically increase in response to inflammation. Despite the hepatic inflammation present in *Atp7b*$^{-/-}$ mice, this protein was downregulated in their plasma compared to WT. During inflammation, AACT inhibits several serine proteases including cathepsin G. Cathepsin G is released at the site of inflammation, where it contributes to defence against pathogens, tissue remodelling, and inflammation. Excessive or prolonged cathepsin G activity, caused by insufficient serpin regulation, can result in tissue damage.[31,32] Accordingly, AACT deficiency has been linked to chronic liver disease and cirrhosis (in a similar manner to alpha-1 antitrypsin deficiency).[32,33] Thus, the reduction of AACT levels in *Atp7b*$^{-/-}$ mice may contribute to (or modulate) hepatic injury during disease progression.

Finally, to examine the translational value of the seven plasma proteins found to be deregulated in the *Atp7b*$^{-/-}$ mouse model, the French National Centres for WD recruited 20 patients. At the time of plasma collection, all WD patients were receiving a continuous treatment (penicillamine, triethylenetetramine or zinc sulfate) and their liver function had normalised. Ideally, we would have liked to include samples from drug-naïve patients (at the time of diagnosis), but given the low incidence of WD, no such samples were available within the time-frame for our study. Consequently, a limitation of this study is that protein changes related to copper overload and hepatic injury could not be explored using the available cohort. Nevertheless, the modifications directly triggered by the perturbed ATP7B function (such as the effects on ceruloplasmin plasma levels) could be investigated using these plasma samples. Following the targeted proteomics study of human plasma samples, it seems possible that the changes associated with murine disease progression may be switched off by chelator treatment in human WD patients. Indeed, only ceruloplasmin (the known biomarker) and alpha-1-antichymotrypsin were confirmed as deregulated in WD patients receiving treatment compared to healthy donors. Other potential reasons for the discrepancy between the human and mouse data may include dissimilar stages of the pathology development, at which samples were analyzed, and a significant regenerative capacity of mouse liver that is evident in older *Atp7b*$^{-/-}$ mice. These results are a clear demonstration of the importance of validating results obtained in animal models as they may not always directly translate to human disease.

Our results confirmed the marked drop in ceruloplasmin plasma concentrations specifically in treated WD patients, in line with an impact of ATP7B dysfunction on accelerated ceruloplasmin clearance. Indeed, impairment of cooper incorporation into apo-ceruloplasmin results in the secretion of a protein that lacks any ferroxidase activity and is rapidly degraded in plasma.[34] No such decrease was observed in the *Atp7b*$^{-/-}$ mouse model, although ceruloplasmin-mediated oxidase activity was previously shown to be markedly reduced in this model (due to the secretion of catalytically inactive apo-ceruloplasmin).[13] This result suggests that the murine apo-ceruloplasmin is much more stable in plasma than the human protein. A more extensive investigation of alpha-1 antichymotrypsin in WD patients would be of interest. Plasma levels of this protein were significantly decreased in treated WD patients compared to healthy controls, and the difference between WD and NASH patients was close to the significance threshold (p-value = 0.09) in the small cohort available for this study. As copper deficiency has been associated with NASH,[35] these results suggest that alpha-1 antichymotrypsin plasma levels could be modulated by copper balance.

Conclusions

This study combined LFQ discovery proteomics and SRM-based targeted proteomics to identify plasma proteome modifications associated with disease development in an established model of hepatic WD, the *Atp7b*$^{-/-}$ mouse. Seven deregulated plasma proteins were identified by the efficient analytical workflow developed. These proteins provide new insights into the pathogenic mechanisms associated with disease progression in this mouse model. Plasma samples from drug-naïve WD patients could reveal further correlations, but for the moment further study should focus on one of these proteins, alpha-1-antichymotrypsin, which showed a similar differential expression pattern in the treated WD patients available here.

Conflicts of interest

There are no conflicts to declare.

Acknowledgements

We thank the team at EDyP for scientific discussions. We are grateful to Prof. Svetlana Lutsenko and Dr Dominik Huster for kindly providing access to the *Atp7b*$^{-/-}$ mouse model, to Samuel Wieczoreck, Sandrine Miesch-Fremy and Khémary Um for technical support, to Fonds de Dotation Clinatec for fundraising support and to Maighread Gallagher-Gambarelli for editing services. This study was supported by grants from the CEA, from the Fondation de la Chimie, from the "Investissement d'Avenir Infrastructures Nationales en Biologie et Santé" programme (ProFI project, ANR-10-INBS-08) and from the French National Research Agency (GRAL project, ANR-10-LABX-49-01).

References

1 A. Poujois and F. Woimant, Wilson's disease: A 2017 update, *Clin. Res. Hepatol. Gastroenterol.*, 2018, **42**(6), 512–520.
2 N. M. Hasan, A. Gupta, E. Polishchuk, C. H. Yu, R. Polishchuk, O. Y. Dmitriev and S. Lutsenko, Molecular events initiating exit of a copper-transporting ATPase ATP7B from the trans-Golgi network, *J. Biol. Chem.*, 2012, **287**, 36041–36050.
3 E. A. Roberts and M. L. Schilsky, Diagnosis and treatment of Wilson disease: an update, *Hepatology*, 2008, **47**, 2089–2111.
4 S. El Balkhi, J. M. Trocello, J. Poupon, P. Chappuis, F. Massicot, N. Girardot-Tinant and F. Woimant, Relative exchangeable copper: a new highly sensitive and highly specific biomarker for Wilson's disease diagnosis, *Clin. Chim. Acta*, 2011, **412**, 2254–2260.
5 S. Heissat, A. Harel, K. Um, A. S. Brunet, V. Hervieu, O. Guillaud, J. Dumortier, A. Lachaux, E. Mintz and M. Bost, Evaluation of the accuracy of exchangeable copper and relative exchangeable copper (REC) in a mouse model of Wilson's disease, *J. Trace Elem. Med. Biol.*, 2018, **50**, 652–657.
6 D. A. Kieffer and V. Medici, Wilson disease: At the crossroads between genetics and epigenetics-A review of the evidence, *Liver Res.*, 2017, **1**, 121–130.
7 T. Lv, X. Li, W. Zhang, X. Zhao, X. Ou and J. Huang, Recent advance in the molecular genetics of Wilson disease and hereditary hemochromatosis, *Eur. J. Med. Genet.*, 2016, **59**, 532–539.

8 V. Medici and K. H. Weiss, Genetic and environmental modifiers of Wilson disease, *Handb. Clin. Neurol.*, 2017, **142**, 35–41.
9 S. Jung, J. R. Whiteaker, L. Zhao, H. W. Yoo, A. G. Paulovich and S. H. Hahn, Quantification of ATP7B Protein in Dried Blood Spots by Peptide Immuno-SRM as a Potential Screen for Wilson's Disease, *J. Proteome Res.*, 2017, **16**, 862–871.
10 O. I. Buiakova, J. Xu, S. Lutsenko, S. Zeitlin, K. Das, S. Das, B. M. Ross, C. Mekios, I. H. Scheinberg and T. C. Gilliam, Null mutation of the murine ATP7B (Wilson disease) gene results in intracellular copper accumulation and late-onset hepatic nodular transformation, *Hum. Mol. Genet.*, 1999, **8**, 1665–1671.
11 S. Lutsenko, Atp7b-/- mice as a model for studies of Wilson's disease, *Biochem. Soc. Trans.*, 2008, **36**, 1233–1238.
12 D. Huster, T. D. Purnat, J. L. Burkhead, M. Ralle, O. Fiehn, F. Stuckert, N. E. Olson, D. Teupser and S. Lutsenko, High copper selectively alters lipid metabolism and cell cycle machinery in the mouse model of Wilson disease, *J. Biol. Chem.*, 2007, **282**, 8343–8355.
13 D. Huster, M. J. Finegold, C. T. Morgan, J. L. Burkhead, R. Nixon, S. M. Vanderwerf, C. T. Gilliam and S. Lutsenko, Consequences of copper accumulation in the livers of the Atp7b-/- (Wilson disease gene) knockout mice, *Am. J. Pathol.*, 2006, **168**, 423–434.
14 M. Ilies, C. A. Iuga, F. Loghin, V. M. Dhople, T. Thiele, U. Volker and E. Hammer, Data on the impact of the blood sample collection methods on blood protein profiling studies, *Data Brief*, 2017, **14**, 313–319.
15 M. Ilies, C. A. Iuga, F. Loghin, V. M. Dhople, T. Thiele, U. Volker and E. Hammer, Impact of blood sample collection methods on blood protein profiling studies, *Clin. Chim. Acta*, 2017, **471**, 128–134.
16 J. Lan, A. Nunez Galindo, J. Doecke, C. Fowler, R. N. Martins, S. R. Rainey-Smith, O. Cominetti and L. Dayon, Systematic Evaluation of the Use of Human Plasma and Serum for Mass-Spectrometry-Based Shotgun Proteomics, *J. Proteome Res.*, 2018, **17**, 1426–1435.
17 J. R. Wisniewski and M. Mann, Consecutive proteolytic digestion in an enzyme reactor increases depth of proteomic and phosphoproteomic analysis, *Anal. Chem.*, 2012, **84**, 2631–2637.
18 J. A. Vizcaino, A. Csordas, N. Del-Toro, J. A. Dianes, J. Griss, I. Lavidas, G. Mayer, Y. Perez-Riverol, F. Reisinger, T. Ternent, Q. W. Xu, R. Wang and H. Hermjakob, 2016 update of the PRIDE database and its related tools, *Nucleic Acids Res.*, 2016, **44**, 11033.
19 S. Wieczorek, F. Combes, C. Lazar, Q. Giai Gianetto, L. Gatto, A. Dorffer, A. M. Hesse, Y. Coute, M. Ferro, C. Bruley and T. Burger, DAPAR & ProStaR: software to perform statistical analyses in quantitative discovery proteomics, *Bioinformatics*, 2017, **33**, 135–136.
20 V. A. Fusaro, D. R. Mani, J. P. Mesirov and S. A. Carr, Prediction of high-responding peptides for targeted protein assays by mass spectrometry, *Nat. Biotechnol.*, 2009, **27**, 190–198.
21 B. MacLean, D. M. Tomazela, N. Shulman, M. Chambers, G. L. Finney, B. Frewen, R. Kern, D. L. Tabb, D. C. Liebler and M. J. MacCoss, Skyline: an open source document editor for creating and analyzing targeted proteomics experiments, *Bioinformatics*, 2010, **26**, 966–968.
22 S. Materia, M. A. Cater, L. W. Klomp, J. F. Mercer and S. La Fontaine, Clusterin (apolipoprotein J), a molecular chaperone that facilitates degradation of the copper-ATPases ATP7A and ATP7B, *J. Biol. Chem.*, 2011, **286**, 10073–10083.
23 A. Poujois and F. Woimant, Challenges in the diagnosis of Wilson disease, *Ann. Transl. Med.*, 2019, **7**, S67.
24 U. Merle, S. Tuma, T. Herrmann, V. Muntean, M. Volkmann, S. G. Gehrke and W. Stremmel, Evidence for a critical role of ceruloplasmin oxidase activity in iron metabolism of Wilson disease gene knockout mice, *J. Gastroenterol. Hepatol.*, 2010, **25**, 1144–1150.
25 H. Hayashi, M. Yano, Y. Fujita and S. Wakusawa, Compound overload of copper and iron in patients with Wilson's disease, *Med. Mol. Morphol.*, 2006, **39**, 121–126.
26 I. P. Trougakos, The molecular chaperone apolipoprotein J/clusterin as a sensor of oxidative stress: implications in therapeutic approaches - a mini-review, *Gerontology*, 2013, **59**, 514–523.
27 S. Materia, M. A. Cater, L. W. Klomp, J. F. Mercer and S. La Fontaine, Clusterin and COMMD1 independently regulate degradation of the mammalian copper ATPases ATP7A and ATP7B, *J. Biol. Chem.*, 2012, **287**, 2485–2499.
28 Y. Li, M. Zalzala, K. Jadhav, Y. Xu, T. Kasumov, L. Yin and Y. Zhang, Carboxylesterase 2 prevents liver steatosis by modulating lipolysis, endoplasmic reticulum stress, and lipogenesis and is regulated by hepatocyte nuclear factor 4 alpha in mice, *Hepatology*, 2016, **63**, 1860–1874.
29 M. A. Ruby, J. Massart, D. M. Hunerdosse, M. Schonke, J. C. Correia, S. M. Louie, J. L. Ruas, E. Naslund, D. K. Nomura and J. R. Zierath, Human Carboxylesterase 2 Reverses Obesity-Induced Diacylglycerol Accumulation and Glucose Intolerance, *Cell Rep.*, 2017, **18**, 636–646.
30 C. Heit, B. C. Jackson, M. McAndrews, M. W. Wright, D. C. Thompson, G. A. Silverman, D. W. Nebert and V. Vasiliou, Update of the human and mouse SERPIN gene superfamily, *Hum. Genomics*, 2013, **7**, 22.
31 C. Baker, O. Belbin, N. Kalsheker and K. Morgan, SERPINA3 (aka alpha-1-antichymotrypsin), *Front. Biosci.*, 2007, **12**, 2821–2835.
32 J. P. Faber, W. Poller, K. Olek, U. Baumann, J. Carlson, B. Lindmark and S. Eriksson, The molecular basis of alpha 1-antichymotrypsin deficiency in a heterozygote with liver and lung disease, *J. Hepatol.*, 1993, **18**, 313–321.
33 L. Ortega, F. Balboa and L. Gonzalez, alpha(1)-Antichymotrypsin deficiency associated with liver cirrhosis, *Pediatr. Int.*, 2010, **52**, 147–149.
34 N. E. Hellman, S. Kono, G. M. Mancini, A. J. Hoogeboom, G. J. De Jong and J. D. Gitlin, Mechanisms of copper incorporation into human ceruloplasmin, *J. Biol. Chem.*, 2002, **277**, 46632–46638.
35 A. Morrell, S. Tallino, L. Yu and J. L. Burkhead, The role of insufficient copper in lipid synthesis and fatty-liver disease, *IUBMB Life*, 2017, **69**, 263–270.